Development 129, 2977-2986 (2002)
Printed in Great Britain © The Company of Biologists Limited 2002
DEV3634

PTHrP and Indian hedgehog control differentiation of growth plate chondrocytes at multiple steps

Tatsuya Kobayashi[1], Ung-il Chung[1], Ernestina Schipani[1], Michael Starbuck[2], Gerard Karsenty[2], Takenobu Katagiri[1,†], Dale L. Goad[1,‡], Beate Lanske[1,§] and Henry M. Kronenberg[1,*]

[1]Endocrine Unit, Massachusetts General Hospital, Boston, MA 02114, USA
[2]Department of Human and Molecular Genetics, Baylor College of Medicine, Houston, TX 77030, USA
[†]Present address: Department of Biochemistry, School of Dentistry, Showa University, Japan
[‡]Present address: Department of Pathology Angell Memorial Animal Hospital, Boston, MA, USA
[§]Present address: Department of Oral Biology, Forsyth Institute, Boston, MA, USA
*Author for correspondence (e-mail: kronenberg.henry@mgh.harvard.edu)

Accepted 20 March 2002

SUMMARY

In developing murine growth plates, chondrocytes near the articular surface (periarticular chondrocytes) proliferate, differentiate into flat column-forming proliferating cells (columnar chondrocytes), stop dividing and finally differentiate into hypertrophic cells. Indian hedgehog (Ihh), which is predominantly expressed in prehypertrophic cells, stimulates expression of parathyroid hormone (PTH)-related peptide (PTHrP) which negatively regulates terminal chondrocyte differentiation through the PTH/PTHrP receptor (PPR). However, the roles of PTHrP and Ihh in regulating earlier steps in chondrocyte differentiation are unclear. We present novel mouse models with PPR abnormalities that help clarify these roles. In mice with chondrocyte-specific PPR ablation and mice with reduced PPR expression, chondrocyte differentiation was accelerated not only at the terminal step but also at an earlier step: periarticular to columnar differentiation. In these models, upregulation of Ihh action in the periarticular region was also observed. In the third model in which the PPR was disrupted in about 30% of columnar chondrocytes, Ihh action in the periarticular chondrocytes was upregulated because of ectopically differentiated hypertrophic chondrocytes that had lost PPR. Acceleration of periarticular to columnar differentiation was also noted in this mouse, while most of periarticular chondrocytes retained PPR signaling. These data suggest that Ihh positively controls differentiation of periarticular chondrocytes independently of PTHrP. Thus, chondrocyte differentiation is controlled at multiple steps by PTHrP and Ihh through the mutual regulation of their activities.

Key words: PTHrP, PTH/PTHrP receptor, Indian hedgehog, Growth plate, Chondrocyte differentiation, Cre-loxP, Mouse

INTRODUCTION

Developing murine growth plates comprise at least three morphologically distinct groups of chondrocytes (see Fig. 3C): round periarticular chondrocytes, flat columnar chondrocytes and hypertrophic chondrocytes. Periarticular chondrocytes proliferate and differentiate into columnar chondrocytes that proliferate further and form orderly columns. Unlike the round periarticular chondrocytes, the flat columnar chondrocytes form columns with clearly defined polarity; this polarity is particularly important in the asymmetric lengthening of the long bones of the limbs. These cells stop proliferating and then differentiate into non-proliferating hypertrophic cells. This sequential and synchronized differentiation is tightly controlled during endochondral bone development; consequently, sharp borders separate the exclusive domains of these three types of cells. One of the major regulators of this differentiation is parathyroid hormone (PTH)-related protein (PTHrP) expressed in the periarticular region. Both PTHrP null (*Pthrp*$^{-/-}$; *Pthlh* – Mouse Genome Informatics) and PTH/PTHrP receptor (PPR) null (*Ppr*$^{-/-}$; *Pthr* – Mouse Genome Informatics) mice develop chondrodysplasia because of premature hypertrophic differentiation (Karaplis et al., 1994; Lanske et al., 1996). The columnar layer is short in *Pthrp*$^{-/-}$ mice and virtually absent in *Ppr*$^{-/-}$ mice.

PTHrP expression in the periarticular region depends upon and is upregulated by another factor that is crucial for cartilage development, Indian hedgehog (Ihh) (Vortkamp et al., 1996; Lanske et al., 1996; Chung et al., 1998; St-Jacque et al., 1999; Chung et al., 2001). In addition to stimulating PTHrP expression, Ihh expression is associated with PTHrP-independent chondrocyte proliferation (Karp et al., 2000).

Previous studies using chimeric growth plates comprising wild-type and PPR-null cells have demonstrated that loss of PPR signaling in proliferating chondrocytes caused premature hypertrophic differentiation (Chung et al., 1998). However, *Ppr*$^{-/-}$ cells in the periarticular region of the chimeric growth plate are not morphologically distinct from wild-type cells. The

possible influence of PPR signaling on the differentiation of periarticular chondrocytes to columnar chondrocytes is, therefore, unclear.

To understand better how PTHrP and Ihh signaling regulate chondrocyte differentiation, we have developed mice with PPR ablation in chondrocytes using the Cre-loxP system (Pluck, 1996). During generation of floxed mice, we also established a mouse line with reduced PPR expression. Through the analysis of these novel mouse models with abnormal PPR signaling, we show that loss or impairment of PPR signaling is associated with chondrocyte differentiation not only at the terminal step but also at an earlier step. In another model with mosaic ablation of the PPR in the growth plate, we show that the differentiation of early chondrocytes is correlated with Ihh action but is not directly regulated by PTHrP. Based on these findings, we propose a model in which PTHrP and Ihh control chondrocyte differentiation at multiple steps.

MATERIALS AND METHODS

Construction of a PPR targeting vector

The targeting vector was designed to introduce two *loxP* sequences and a neomycin resistant gene (*neo*) to generate a floxed PPR allele for gene inactivation by *Cre* recombinase (Sauer, 1993). The *loxP* sites are placed in the introns flanking the essential E1 exon. A *neo* is placed adjacent to the first *loxP* site and an exogenous *Hin*dIII site is placed at the second *loxP* site (Fig. 1A). A thymidine kinase (*tk*) cassette is placed outside of the homologous sequence. The PPR genomic clones were isolated from a DashII 129/SvJ mouse liver genomic library using a rat PPR cDNA probe (Lanske et al., 1996). Two *loxP* sequences were inserted into a *Bam*HI/*Kpn*I PPR gene fragment containing exon E1 at the *Bgl*II and *Sac*I sites. An MC-1 *neo* cassette (kindly provided by Dr S. Dymecki) was placed adjacent to the first *loxP* site. A *Xba*I/*Bam*HI fragment and a *Kpn*I/*Hin*dIII fragment, both adjacent to the *Bam*HI/*Kpn*I fragment in the PPR gene, were ligated to the modified *Bam*HI/*Kpn*I fragment to reconstitute the 7.5 kb of the PPR genomic sequence spanning the floxed exon E1 and exon E2. The *tk* cassette, derived from the pPNT vector (Karaplis et al., 1994) was placed at the 3′ end of the construct.

Transfection of ES cells and generation of PPR floxed mice

*Not*I-linearlized vector was transfected into J1 ES cells by electroporation. ES cells were selected with G418 (250 μg/ml) and gancyclovir (2 μM). Doubly resistant colonies were subjected to Southern blot analysis. Homologous recombinants were diagnosed by Southern hybridization using the 5′-external probe A (Fig. 1A) after *Hin*dIII digestion of the ES cell genomic DNA. Homologous recombinants showed a mutant 8.5 kb band and a 10 kb band corresponding to the wild-type allele. Homologous recombination at the 3′ side of the targeting vector was also confirmed by Southern hybridization using 3′-external probe B after *Xho*I digestion. Homologous recombinants had a 6 kb band that corresponded to the mutant allele. Several ES cell lines were injected into C57BL/6 blastocysts for generation of chimeric mice. Chimeric mice were crossed with C57BL/6 mice to establish F_1 lines. Three independent lines were established. One of them (line FL23) exhibited an unexpected mutation in the PPR locus, as described in the text.

Generation of Cre transgenic mice

Col2-Cre transgenic mice where Cre recombinase (O'Gorman et al., 1997) is expressed under the rat collagen type II promoter (Yamada, 1990) were generated as described elsewhere (Schipani et al., 2001). Ost-Cre transgenic mice bear a fusion gene composed of a 1.3 kb fragment of the mouse OG2 promoter (Ferendo et al., 1998) fused to Cre recombinase and polyA signal excised from a pCBM-9 vector (Saur and Henderson, 1989). After removing vector sequence, DNA was subjected to pronuclear injection. *Cre* activity was assessed using Rosa26-R (R26R) reporter mice (Soriano, 1999): *Cre* transgenic mice were crossed with R26R mice. Embryos were collected, fixed and stained with X-gal, as described elsewhere (Chung et al., 1998).

Genotyping of mice

The floxed PPR allele and the unanticipated *d* allele were analyzed by PCR using primers P1 (5′-TGGACGCAGACGATGTCTTTACCA-3′) and P2 (5′-ACATGGCCATGCCTGGGTCTGAGA-3′), which recognize the sequences spanning the 3′ *loxP* site. Wild-type and mutant alleles give 450 bp and 490 bp PCR products, respectively. The PPR null locus was detected using PCR primers, P3 (5′-CCA-CCAATGTGAGTTCCTACAGAAA-3′) for an intronic sequence between exons E2 and E3, and P4 (5′-TCCAGACTGCCTTGGG-AAAAGCGC-3′) for the PGK promoter used for the neomycin resistant marker. The mutant allele with a retained PGK promoter sequence gives a 500 bp band. *Cre* sequences were detected by PCR using primers recognizing internal sequence of the transgene (P5, 5′-CGCGGTCTGGCAGTAAAAACTATC-3′; P6, 5′-CCCACCGTC-AGTACGTGAGATATC-3′). All PCR reactions used the following program: 94°C for 10 minutes, followed by 35 cycles of 95°C for 30 seconds, 68°C for 30 seconds, and 72°C for 1 minute.

Southern and northern blotting

DNA was prepared from the livers of mice homozygous for the wild-type PPR, the floxed PPR and the mutated PPR described in the text. After overnight enzyme digestion, DNA was separated in 0.7% agarose gels, denatured and transferred onto nylon or nitrocellulose membranes.

Total RNA was extracted from the kidneys of 3-week-old mice. RNA was separated in a 1% agarose gel and transferred onto a nitrocellulose membrane. The probe for the mouse PPR was generated by a random priming method (Megaprime, Amersham), using the DNA template amplified from mouse kidneys by RT-PCR using primers P7 (5′-ACCAACTACTACTGGATTCTGGTGG-3′) and P8 (5′-CGGCTCCAAGACTTCCTAATCTCTG-3′). The probes used for Southern analysis are indicated in Fig. 1A. RNA and DNA hybridization was performed using the QuickHyb Kit (Stratagene) according to the manufacturer's instruction. Signals were visualized on X-ray films or by the Cyclone storage phosphor system (Packard). PPR and GAPDH mRNA were quantified using the Cyclone storage phosphor system. PPR mRNA levels normalized for GAPDH mRNA were compared. The band intensity of the Southern analysis was similarly quantified and normalized with the *Gapdh* gene. The normalized band intensities obtained from at least three independent blots for each set were used for the comparisons.

PPR cDNA sequencing

Total RNA was prepared from the kidney of homozygous *d/d* mutant mice. Reverse transcription was performed using Superscript reverse transcriptase (Gibco/BRL) followed by PCR using primers P9 (5′-CCGAGGGACGCGGCCCTAG-3′) and P10 (5′-AGTCCTGAATA-GACAGCCAGCCAAA-3′) to amplify the entire coding sequence of the PPR. DNA sequence was determined by direct sequencing bi-directionally using the following sequencing primers: forward primers, P9, P11 (5′-GCTGCTCAAGGAAGTTCTGCACACA-3′), P12 (5′-GATCTACACCGTGGGATATTCCATG-3′), P13 (5′-ACCA-ACTACTACTGGATTCTGGTGG-3′), P14 (5′-CACTGTGGCAG-ATCCAGATGCACTA-3′); backward primers, P10, P14 (5′-CGG-CTCCAAGACTTCCTAATCTCTG-3′), P15 (5′-AGTGTTGGCCA-AGGTTGCTCTGACA-3′), P16 (5′-GCAGCATAAACGACAGGA-ACATGTG-3′), P17 (5′-CAGCAAACGATGTTGTCCCACTCTG-3′).

In situ hybridization

Tissues were fixed in 4% paraformaldehyde/PBS overnight at 4°C, processed, embedded in paraffin wax and cut. Sections were stained with H&E or nuclear Fast Red (Vector laboratories). In situ hybridization was performed as described previously (Lee et al., 1995) by using complimentary ^{35}S-labeled riboprobes. The probes for mouse type X collagen, mouse patched 1, mouse Ihh and rat PTHrP were obtained from Dr Bjorn Olsen (Harvard Medical School), Dr Ron Johnson (Stanford University, Stanford) Dr Benoit St-Jacques (Harvard University) and Dr Andrew C. Karaplis (McGill University), respectively. Rat full-length PPR cDNA probe, R15B has been described previously (Calvi et al., 2001). An exon E1 specific PPR probe was generated by PCR using primers: F, 5′-GTGGACG-CAGACGATGTCTTTACC-3′; and R, 5′-CTGCTGTGTGCAGAA-CTTCCTTGA-3′. PCR product was subcloned into pGEMT Easy vector (Promega).

BrdU labeling

Pregnant mice received intra-peritoneal injections of 50 μg BrdU/g of body weight and were sacrificed 1 or 24 hours later. Limbs were dissected and fixed in 4% paraformaldehyde overnight at 4°C. Tissues were processed, embedded and sectioned using standard procedures. BrdU was detected using a BrdU Staining Kit (Zymed Laboratories). The BrdU-positive and -negative nuclei were counted in the periarticular region and the columnar region separately. The border between the periarticular and columnar regions was defined as the line separating these two morphologically distinct groups of chondrocytes.

For counting of BrdU-positive cells in the periarticular region, using sections with smaller periarticular regions, we first determined an area for BrdU counting by drawing a closed line that made the area as large as possible, while avoiding the border containing ambiguous cells. Then, we applied the same area on the control sections as it was placed in the center of the corresponding region. We confirmed that the area only included cells with the typical morphological appearance of periarticular chondrocytes. For counting of BrdU-positive cells in the columnar region, as $Ppr^{d/-}$ growth plates lack sharp transition of between columnar and hypertrophic regions, we first chose top one third of the columnar region of $Ppr^{d/-}$ mice not to include any hypertrophic cells. We set a rectangular area excluding periarticular and perichondrial cells for BrdU counting. The same rectangle was applied onto control sections. Exclusion of other types of cells was similarly confirmed.

Mutants and controls used in this study were littermates. Nine sections from at least three independent mice per group were counted. Statistical analysis was done by ANOVA.

RESULTS

Generation of PPR floxed mice and mice with decreased PPR

For the generation of mice with insertion of loxP sequences (floxed mice), a targeting vector was designed with loxP sequences in introns flanking the essential E1 exon of the PPR gene (Fig. 1A). Floxed mice were crossed with $Ppr^{+/-}$ mice to generate compound heterozygous mice, in which one PPR allele was disrupted and the other was mutated by *neo-loxP* targeting. The compound heterozygous mice from two independent lines were phenotypically normal. However, mice from one floxed line developed growth retardation and deformity of the limbs postnatally. Homozygous mice for this mutated allele appeared grossly normal. Because the growth retardation over multiple matings and generations invariably appeared in mice carrying the mutated PPR gene opposite an ablated PPR gene, we concluded that the mutant PPR gene was closely linked to and probably responsible for the phenotype. We, hereafter, designate this mutant allele '*d*' for damaged PPR allele. In situ hybridization for the PPR mRNA in the cartilage of 3-week-old mice revealed decreased expression of PPR mRNA, but the expression pattern was preserved (Fig. 1B). PPR transcripts of normal length were produced in the mutant mice with reduced expression level, determined by northern blot analysis using kidney RNA prepared from homozygous mice (Fig. 1C). Direct sequence of RT-PCR products from homozygous mouse kidney RNA revealed that the transcripts had a normal coding sequence (data not shown). A series of Southern analyses were performed using homozygous mouse DNA to analyze the abnormality of the *Ppr* gene in the d allele (Fig. 1D-K). Three copies of the targeting vector are inserted in the targeted locus through homologous recombination. This was accompanied by replacement of the endogenous sequence (determined by PCR using P1 and P2 primers; data not shown), an amplification of endogenous sequence immediately 5′ of the targeted region and an insertion of a tk cassette. A possible model for the *d Ppr* gene is shown in Fig. 1L.

Mice with chondrocyte-specific PPR ablation have a growth plate phenotype similar to that of *Ppr*-null mice

Homozygous floxed, $Ppr^{fl/fl}$ mice and compound heterozygous $Ppr^{fl/-}$ mice have no abnormality in growth plate cartilage (data not shown). Chondrocyte-specific *Ppr* gene ablation was carried out by mating these floxed mice with *Cre* transgenic mice expressing *Cre* under the control of the rat type II collagen promoter (*Col2-Cre*). *Cre* activity was determined using R26R reporter mice, and was present in growth plate chondrocytes but limited to the chondrocytes and a part of the perichondrium, intra-joint tissues, ligaments and tendons (Fig. 2A). PPR is predominantly expressed in the prehypertrophic region and weakly in columnar chondrocytes (Fig. 2J). PPR expression determined by an exon E1-specific probe was lost in the growth plate of double mutant mice, $Col2\text{-}Cre{:}Ppr^{fl/fl}$ (Fig. 2K). $Col2\text{-}Cre{:}Ppr^{fl/fl}$ mice develop chondrodysplasia that resembles that of $Ppr^{-/-}$ (Fig. 2B,C): the tibial growth plate is shortened and lacks most of the columnar chondrocytes. Reduction on the proliferating chondrocytes with preservation of a fairly normal hypertrophic layer was confirmed by the expression patterns of type II and type X collagens (Fig. 2D-I). The periarticular region is flattened (Fig. 2C). At E16.5, the mutant sternum is mostly occupied by hypertrophic cells, whereas there are few hypertrophic cells in the control (Fig. 2L,M). However, unlike $Ppr^{-/-}$ mice in some genetic backgrounds, mutant mice survive until birth and they are not as small as $Ppr^{-/-}$ mice (data not shown). From these observations, we conclude that the $Ppr^{-/-}$ growth plate phenotype is primarily caused by loss of PPR signaling in the chondrocytes themselves.

Growth plates of $Ppr^{d/-}$ embryos have a phenotype distinct from that of $Ppr^{-/-}$ mice

In contrast to $Ppr^{-/-}$ mice, $Ppr^{d/-}$ mice are born with a reasonably normal appearance and size. Around 7 days of age, they start to show growth retardation and limb deformities (data not shown). To clarify the nature of bone abnormality of $Ppr^{d/-}$ mice, we examined fetal growth plates. One of the most striking features of the tibial growth plates of the E17.5 $Ppr^{d/-}$

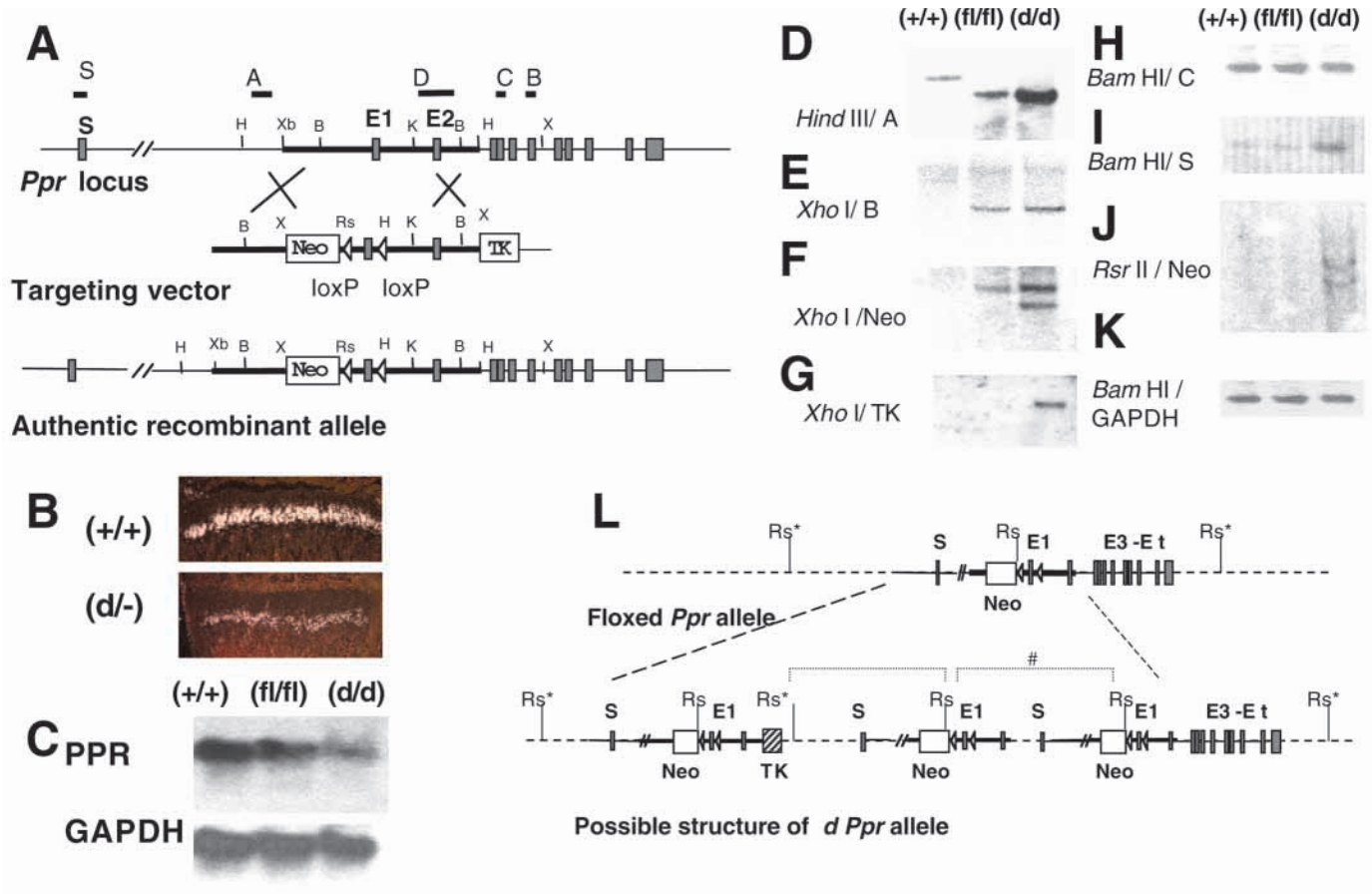

Fig. 1. Generation of floxed and *d* allele of the *Ppr* locus. (A) Schematic representation of the *Ppr* locus, the targeting vector used for floxed allele generation and the floxed (*fl*) locus. Exons and selectable genes are indicated by gray and white boxes, respectively. *loxP* sequences are indicated by open triangles. *Neo* and *tk* cassettes are indicated as Neo and TK, respectively. Restriction enzyme sites for *Bam*HI, *Kpn*I, *Hin*dIII, *Rsr*II, *Xho*I and *Xba*I are indicated as B, K, H, Rs, X and Xb, respectively. Probes used for Southern blot analysis are indicated with bold lines above the corresponding sequences. (B) In situ hybridization of PPR in 3-week-old mouse growth plates. (C) Northern blot analysis of PPR mRNA expression in the kidney of 8-week-old mice. (D-K) Southern blot analysis for the characterization of the *Ppr d* allele. DNA (10 μg) purified from wild type (+/+), homozygous floxed (fl/fl) and homozygous damaged (d/d) mice was digested with indicated restriction enzymes and hybridized with the probes indicated. Probes A and B are external probes in the 5′- and 3′-flanking regions of the targeted sequence, respectively. Probes C and S are exonic sequences for exon E3 and exon S of the *Ppr* gene, respectively. Probes Neo and TK are specific to the *neo* and the *tk* genes, respectively. (D) Only a single 8.5 kb band produced by the homologous recombination at the 5′-end of the targeting vector is seen in both (fl/fl) and (d/d). Note the band intensity of (d/d) is greater than that of (fl/fl), suggesting amplification of the 5′-flanking region. (E) Homologous recombination at the 3′-end was confirmed by an external probe B. Because the band intensities of the (d/d) and (fl/fl) are similar, we conclude that the 3′-flanking region is not amplified. The band in +/+ is not visualized probably because of the large size of the fragment (>18 kb). (F) An extra band for at 6.5 kb is present in d/d, in addition to the expected 8 kb band also seen in (fl/fl). (G) A band for *tk* is present only in d/d. (H) The band intensity for exon E3 is the same among in +/+, fl/fl and d/d. (I) The band intensity for S exon is about three times as intense in d/d as in +/+ or fl/fl. (J) Hybridization with Neo probe after *Rsr*II digestion visualized two bands at 20 kb and 25 kb only in d/d. These may represent tandemly repeated sequences because one of the *Rsr*II bands detected by Neo probe was also detected by probe D, corresponding to the broken bracket marked with # in L (data not shown). Neither of these bands was detected by TK probe (data not shown). (K) Each blot shown above was reprobed with the GAPDH probe for normalization. A representative blot is shown. (L) A possible structural model for the *d* allele of the *Ppr* locus. The *d* allele is likely to contain three copies of the targeting vector. Targeting vectors are integrated into the genome replacing the endogenous sequence of the corresponding region. One copy of *tk* sequence is present. A part of the 5′-flanking sequence including exon S is amplified with the targeting vector. Rs*, unmapped *Rsr*II sites. Broken brackets, possible DNA fragments visualized in H. #, the probable fragment that hybridized with both Neo and D probes in H.

embryo is the expansion of the hypertrophic layer (Fig. 3A,C). The total length of the tibia is slightly greater than that of the control littermates, unlike the tibial length of *Ppr*-null mice. The nature of the expanded layer was characterized by in situ hybridization (Fig. 3B): the reduction of PPR expression in $Ppr^{d/-}$ mice was also present at this age. The type II collagen-expressing domain and the type X collagen-expressing domain have a minimal overlap in the wild-type growth plate, whereas both of the type II and type X collagen-expressing domains are broadened, with an expanded overlap zone in the $Ppr^{d/-}$ growth plate. Similarly, the prehypertrophic domain marked by *Ihh* expression is expanded. The upper part of the expanded hypertrophic layer comprises mostly unmineralized, relatively small hypertrophic cells with abundant extracellular matrix

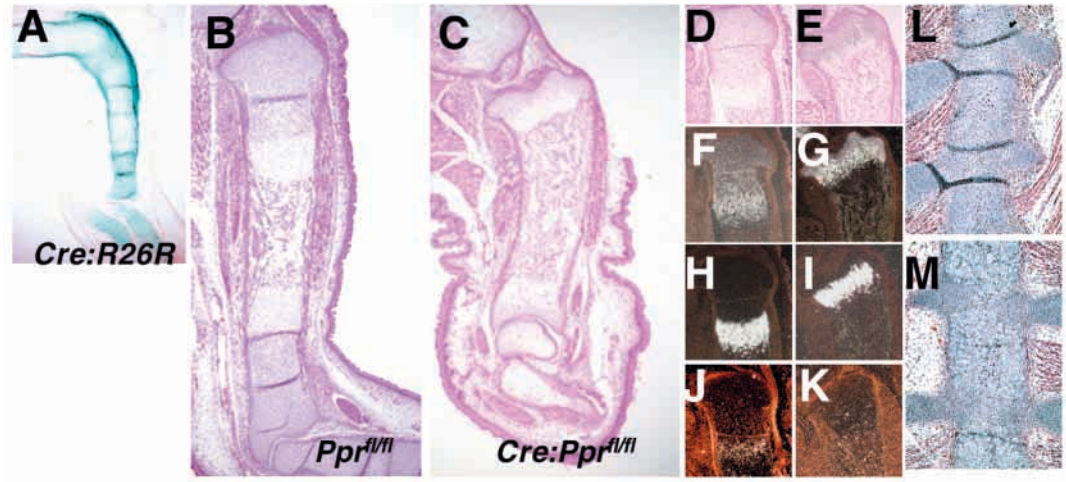

Fig. 2. Cartilage-specific PPR ablation. (A) Tissue-specific activity of *Cre* recombinase. A *Col2-Cre:R26R* doubly transgenic, E15.5 embryo was stained with X-gal to visualize *Cre* activity. As well as chondrocytes, a part of perichondrium, ligaments, tendon and intra-joint tissues are stained blue representing *lacZ* activity. (B-K) Tibia of E17.5 embryos of homozygous floxed mice with (C,E,G,I,K) or without (B,D,F,H,J) *Col2-Cre* gene. (B-E) Bright field views of Hematoxylin and Eosin stained sections. (F-K) Dark field views of in situ hybridization with type II collagen (F,G), type X collagen (H,I) and PPR detected by a specific probe for the E1 exon (J,K). (L,M) The sterna of E 16.5 day-old embryos at the third inter-costal space of $Ppr^{fl/fl}$ (L) and *Col2-Cre:*$Ppr^{fl/fl}$(M). The sternum of the *Col2-Cre:*$Ppr^{fl/fl}$ mice is mostly occupied with hypertrophic chondrocytes.

(Fig. 3C). These hypertrophic cells do not express osteopontin, a marker for mineralized hypertrophic cells and osteoblasts (Fig. 3B). Therefore, the expansion of the hypertrophic layer is mostly due to an increase in early hypertrophic cells. The columnar region, as well as the periarticular region of $Ppr^{d/-}$ growth plates, is slightly, but consistently, smaller than that of controls (indicated by brackets in Fig. 3C).

To support the hypothesis further that reduced PPR signaling in chondrocytes is responsible for the cartilage phenotype of $Ppr^{d/-}$ mice, we crossed $Ppr^{d/-}$ mice with transgenic mice that express a constitutively active *Ppr* mutant gene in chondrocytes using rat type II collagen promoter (*caPpr*). This gene has previously been shown to rescue the growth plate abnormality of $Pthrp^{-/-}$ mice (Schipani et al., 1997). The proximal tibias of E17.5 *caPpr* mice, $Ppr^{d/-}$ mice and *caPpr:*$Ppr^{d/-}$ mice were compared (Fig. 3D). The tibia of the *caPpr* mouse is characterized by an expansion of fully differentiated hypertrophic chondrocytes that express osteopontin and a decreased amount of type X collagen mRNA. Although both the *caPpr* and $Ppr^{d/-}$ mice show expansion of the hypertrophic region, the hypertrophic region of $Ppr^{d/-}$ mice expresses high levels of type X collagen mRNA and little osteopontin mRNA. This characteristic abnormality of the $Ppr^{d/-}$ growth plate disappears when the *caPpr* gene is introduced, and the growth plate of the double mutant mice, *caPpr:*$Ppr^{d/-}$ is indistinguishable from that of *caPpr*.

Impairment or loss of PPR signaling causes acceleration of early chondrocyte differentiation

The number of cells in each chondrocyte layer represents the balance between the number of cells entering and leaving the layer as well as proliferation within the layer. To analyze these steps, first, we performed BrdU labeling (Fig. 4A): when E17.5 mice were sacrificed 1 hour after BrdU administration, no BrdU-positive cells were found in the hypertrophic region either in $Ppr^{d/-}$ or in wild-type controls. The fraction of cells labeled with BrdU in the columnar region was unchanged in $Ppr^{d/-}$ mice. It was, however, significantly increased in the periarticular region of $Ppr^{d/-}$ mice, even though the region was smaller. This was also confirmed in E16.5 and E18.5 mice (data not shown). This suggests that periarticular chondrocytes differentiate into columnar chondrocytes and therefore leave the periarticular region at a greater rate than that of controls. Then, we performed BrdU pulse-chase assay to see whether hypertrophic chondrocytes are also generated at a greater rate in $Ppr^{d/-}$ mice. Proliferating chondrocytes of E17.5 embryos were pulse labeled with BrdU. Mice were sacrificed 24 hours after BrdU labeling. BrdU-positive hypertrophic chondrocytes are generated during the period. We found that those BrdU-positive hypertrophic chondrocyte did not reach chondro-osseous junction at this condition; therefore, we did not lose BrdU-positive hypertrophic chondrocytes by the replacement of cartilage by bone cells. As hypertrophic chondrocytes do not incorporate BrdU (Fig. 4A), these BrdU-positive hypertrophic chondrocytes are generated by differentiation of columnar chondrocytes labeled with BrdU 24 hours before sacrifice. The number of BrdU-positive hypertrophic chondrocytes is determined by the number and proliferation of BrdU-labeled proliferating chondrocytes and the rate of their hypertrophic differentiation. The number of BrdU-positive hypertrophic cells produced in $Ppr^{d/-}$ mice during this time was greater than that of controls, and the area encompassed by BrdU-positive hypertrophic cells was greater (Fig. 4B). As the number and the proliferation rate of columnar chondrocytes of $Ppr^{d/-}$ mice were not greater than the control (Fig. 4A), we concluded that the increased number of BrdU-positive hypertrophic chondrocytes was due to an increase in the rate of hypertrophic differentiation. The observations that osteopontin is only expressed in the terminal end of the hypertrophic region of $Ppr^{d/-}$ mice with no expansion in number of osteopontin-positive cells suggest that this acceleration does not continue in the step of further hypertrophic maturation. Thus,

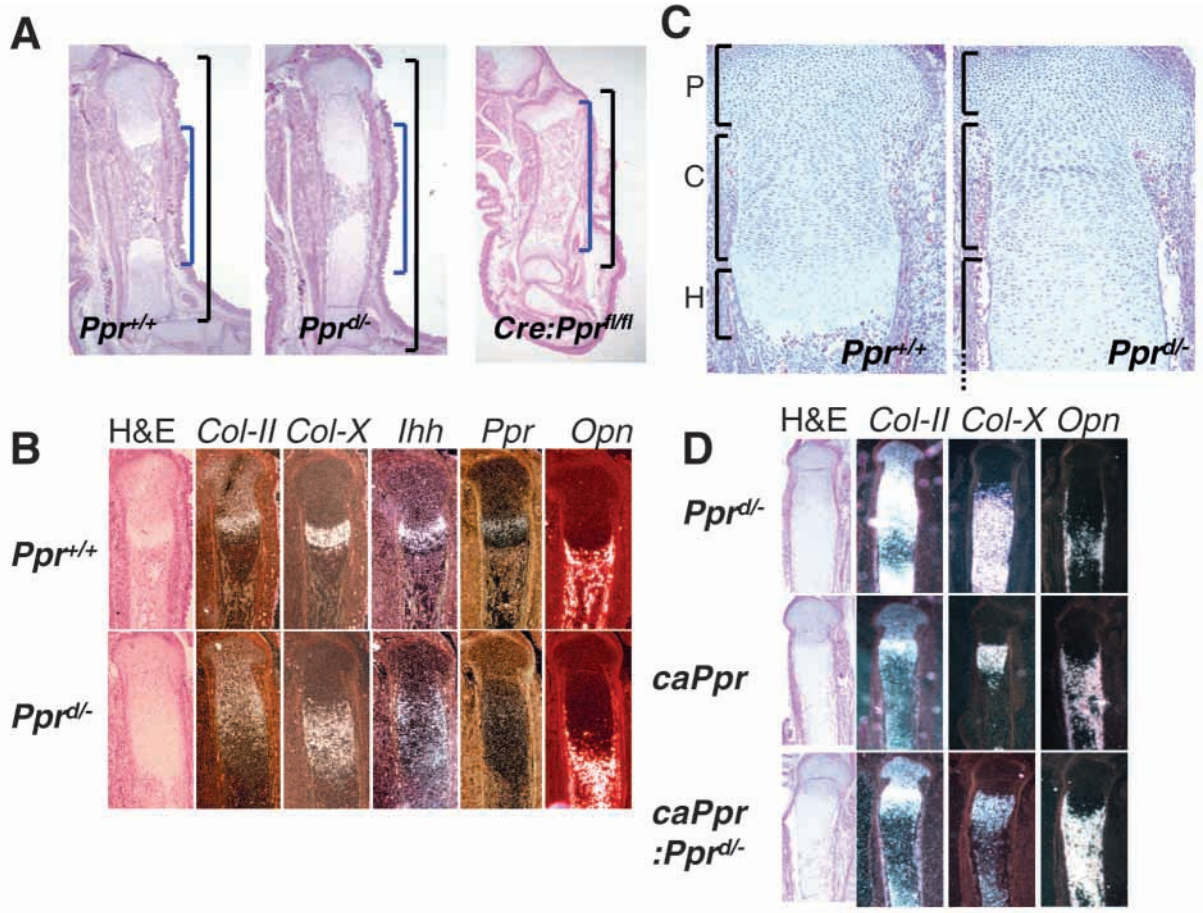

Fig. 3. Growth plates of $Ppr^{d/-}$ mice. (A) Tibia of E17.5 $Ppr^{+/+}$, $Ppr^{d/-}$ and *Col2-Cre:*$Ppr^{fl/fl}$ embryos. The growth plates and the bone length (indicated by black brackets) in the $Ppr^{d/-}$ are greater than in the wild type, whereas they are reduced in the *Col2-Cre:*$Ppr^{fl/fl}$ mouse. Note that the post-proliferating region (the hypertrophic zone and the marrow region that replaced hypertrophic chondrocytes) indicated by the blue brackets is not much different among these animals. (B) Differentiation marker expression in E17.5 embryos. *Col-II*, type II collagen; *Col-X*, type X collagen*; Ihh*, Indian hedgehog; *Ppr*, parathyroid hormone receptor (detected by R15B probe); *Opn*, osteopontin. (C) High-magnification view of growth plates of the E17.5 proximal tibia. In contrast to the great expansion of the hypertrophic region, the periarticular and columnar regions are slightly smaller in the $Ppr^{d/-}$. Brackets indicate the three regions: P, periarticular region; C, columnar region; H, hypertrophic region. (D) *CaPpr* expression overcomes the $Ppr^{d/-}$ phenotype. In situ hybridization of the indicated markers shows the identical patterns between *caPpr* and *caPpr: *$Ppr^{d/-}$ double mutants.

acceleration of the differentiation rate of periarticular into columnar chondrocytes as well as of columnar to hypertrophic chondrocytes appear to have caused an accumulation of early hypertrophic chondrocytes in $Ppr^{d/-}$ mice. The acceleration of periarticular to columnar differentiation was also observed in mice with PPR ablation in chondrocytes of E17.5 mice (Fig. 4C). Despite the decreased size of the periarticular region, chondrocyte proliferation was increased.

Upregulation of Ihh activity is correlated with early chondrocyte differentiation

The PPR is little, if at all, expressed in periarticular chondrocytes. We, therefore, considered other possible mediators of the accelerated differentiation of periarticular chondrocytes in PPR-defective mice. We found that morphological changes of the growth plate in these PPR-defective mice also altered the *Ihh* expression domain (Fig. 5). As Ihh has PTHrP-independent roles in cartilage development, and $Ihh^{-/-}$ mice show marked reduction in proliferation (Karp et al., 2000), we hypothesized that possible upregulation of Ihh action may have caused this acceleration of early chondrocyte differentiation. To test this possibility, we examined expression of patched 1 (*Ptc*; *Ptch* – Mouse Genome Informatics), a marker of Ihh action (Goodrich et al., 1996), and *Pprp* expression (Fig. 5). *Ptc* expression is strongest in the domain adjacent to the *Ihh* domain, fading away towards the articular surface in the $Ppr^{+/+}$ growth plate, whereas its expression in the periarticular region is upregulated in *Col-2Cre: *$Ppr^{fl/fl}$ and $Ppr^{d/-}$ mice. Upregulation of PTHrP expression in the periarticular region also suggests increased Ihh activity in this region.

Ectopic hypertrophic cells expressing Ihh causes acceleration of early chondrocyte differentiation independent of PTHrP

To determine whether Ihh action stimulates differentiation of periarticular to columnar chondrocytes, we introduced ectopic Ihh expression near the periarticular region. For this purpose,

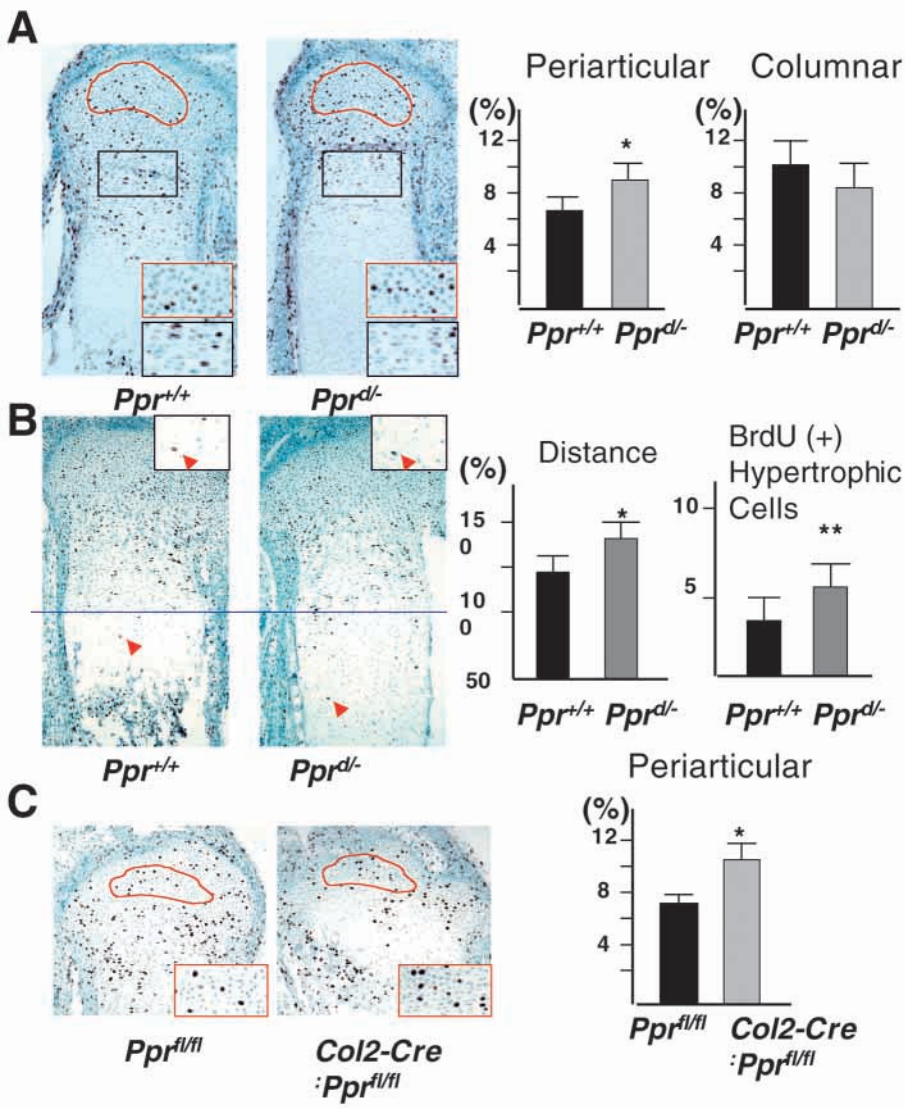

Fig. 4. BrdU labeling analysis. (A) BrdU-positive chondrocytes of E17.5 embryos were counted in the area indicated by red and black lines for the periarticular region and the columnar region, respectively. Insets are magnified views of the periarticular (red outline) and columnar (black outline) regions. The number of BrdU-positive cells was divided by the number of nuclei to calculate proliferation rate (shown on the right). At least nine sections from three animals for each genotype were counted. *, statistically significant by ANOVA with $P<0.05$. (B) BrdU pulse-chase assay. Representative pictures of proximal tibias of mice sacrificed 24 hours after single BrdU injection at E17.5. Hypertrophic cells were identified by morphological criteria. The blue lines indicating the beginning of the hypertrophic zone were drawn by connecting the points at which bone collars started to form. The distance between the lines and the furthest BrdU-positive hypertrophic cells (indicated by red arrowheads), as well as number of BrdU-positive hypertrophic chondrocytes were measured and counted (shown on the right). Insets are magnified views of BrdU-positive hypertrophic cells. The distance was 32% greater in $Ppr^{d/-}$ than in controls. The absolute number of BrdU-positive cells was increased in $Ppr^{d/-}$ by 2. At least ten sections from two independent animals for each genotype were subjected to the analysis. * and **, statistically significant by ANOVA with $P<0.05$ and $P<0.01$, respectively. (C) BrdU labeling ratio was similarly calculated in the periarticular chondrocytes of E17.5 mice with cartilage-specific PPR ablation (shown on the right). Insets are magnified views of the periarticular region. At least nine sections from three independent animals for each genotype were counted. *, statistically significant by ANOVA with $P<0.05$.

we took advantage of a line of Osteocalcin-Cre (*Ost-Cre*) transgenic mice. A reporter experiment showed that 30% of proliferating chondrocytes had Cre activity (Fig. 6A). The activity is primarily limited to the columnar region and barely present in the periarticular region. *Ost-Cre:* $Ppr^{fl/fl}$ mice develop ectopic hypertrophy in the columnar region due to premature hypertrophic differentiation of the cells that have lost the PPR gene (Fig. 6C). These cells express Ihh close to the periarticular region (Fig. 6E), with evidence of increased Ihh signaling in the periarticular region, as indicated by *Ptc* and *Pthrp* upregulation (Fig. 6G,I). The BrdU labeling ratio of the periarticular chondrocytes of E17.5 mice was significantly increased without enlargement of the periarticular region, suggesting acceleration of periarticular chondrocyte differentiation into columnar cells (Fig. 6J). This increase in BrdU labeling ratio of periarticular chondrocytes was also confirmed in E16.5 and E18.5 embryos (data not shown). This acceleration occurs in the presence of increased PTHrP expression (Fig. 6I) with presumably little disruption of the *Ppr* gene in the periarticular region, as Cre activity in this region is minimal. Hence, we conclude that the acceleration of periarticular to columnar cells is not caused directly by loss of PPR of the periarticular chondrocytes.

DISCUSSION

The role of PTHrP signaling through the PPR in chondrocyte differentiation has been demonstrated by analysis of mutant mice missing the genes for these proteins (Karaplis et al., 1994; Lanske et al., 1996) as well as though the use of chimeric mice (Chung et al., 1998; Chung et al., 2001).

The observation that *Col2-Cre:*$Ppr^{fl/fl}$ mice showed a growth plate abnormality similar to that of the $Ppr^{-/-}$ mice is consistent with the previous finding that loss of PPR signaling in columnar chondrocytes per se accelerates their terminal differentiation (Chung et al., 1998). However, chondrocyte-specific *Ppr*-null mice differ from $Ppr^{-/-}$ mice in body size and embryonic lethality. Further, in the $Ppr^{-/-}$ growth plate, the initial hypertrophic differentiation is delayed (Lanske et al., 1999), whereas it is accelerated in chondrocyte-specific *Ppr*-null mice (e.g. Fig. 2J,K). Thus, the loss of the PPR in the

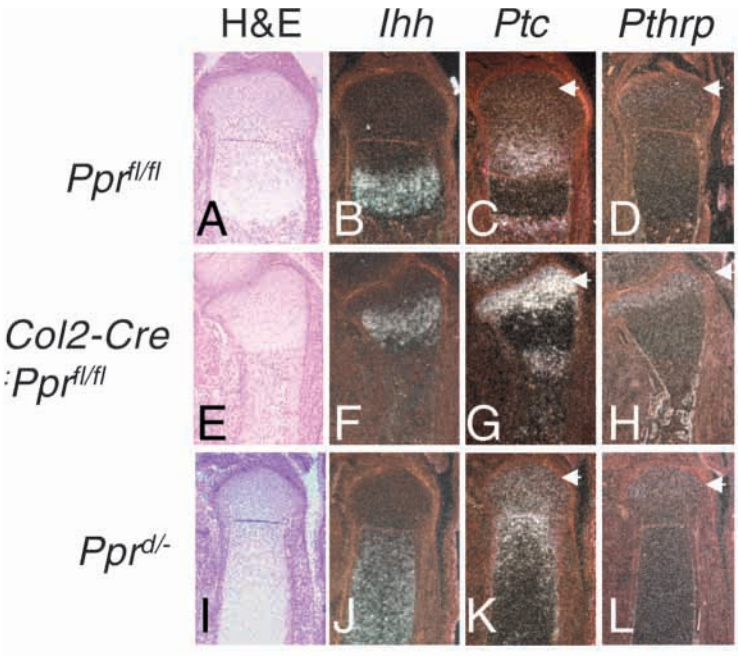

Fig. 5. Ihh signaling activities in periarticular chondrocytes. In situ hybridization for *Ihh* (B,F,J), *Ptc* (C,G,K), *Pthrp* (D,H,L), Hematoxylin and Eosin (A,E,I). (A-D) $Ppr^{fl/fl}$ (control), (E-H) *Col2-Cre:*$Ppr^{fl/fl}$ (I-L) $Ppr^{d/-}$. Arrowheads indicate *Ptc* and *Pprp* expression in the periarticular region.

cartilage as well as in the other tissues contribute to the $Ppr^{-/-}$ growth plate phenotype. Nevertheless, the strong similarities of the cartilage phenotypes seen among $Ppr^{-/-}$, $Pthrp^{-/-}$ and *Col2-Cre:*$Ppr^{fl/fl}$ mice suggests that these phenotypes are primarily caused by the loss of PPR signaling in chondrocytes.

Although universal gene ablation is a powerful method for analyzing the roles of genes in vivo, the extreme nature of the phenotypes can limit conclusions, especially when gene ablation causes early embryonic lethality. Partial knockout (knock-down) of gene expression can, therefore, be revealing. To date, several different methods have been reported to generate mice that have phenotypes due to reduced gene expression or function: transgenic animals that express antisense RNA (Nemir et al., 2000) or dominant negative proteins (Go et al., 2000), introduction of hypomorphic mutation into proteins (Tang et al., 1997) and insertion of foreign sequences into intronic sequences to disturb efficient RNA splicing (Nagy et al., 1998; Meyers et al., 1998; Mohn et al., 1999). The mice with reduced PPR expression presented here were unintentionally obtained during an attempt to generate floxed PPR mice. Although the genetic structure of the *d* allele is not completely understood, the following findings indicate that the phenotypes of $Ppr^{d/-}$ mice are caused by reduction of normal PPR mRNA expression: (1) PPR mRNA expression was reduced, as determined by RNA blot and in situ hybridization analysis; (2) the RT-PCR product had the normal coding sequence of PPR and the mRNA was of normal size; (3) homozygous $Ppr^{d/d}$ mice have milder phenotypes than do $Ppr^{d/-}$ mice (data not shown), a result expected if the *d* allele generates a smaller amount of a normal mRNA; (4) heterozygous $Ppr^{d/+}$ mice are virtually normal (data not shown); and (5) overactivity of the PPR caused by a constitutively active PPR mutation completely reverses the $Ppr^{d/-}$ mutant phenotype. Based on northern blot analysis (Fig. 1B,C and data not shown) and the fact that the $Ppr^{d/d}$ mice have slightly abnormal growth plates while $Ppr^{+/-}$ mice do not have apparent morphologic abnormalities, PPR expression level in $Ppr^{d/-}$ mice is estimated to be less than 50% of that of heterozygous $Ppr^{+/-}$ mice. The growth plate phenotype of $Ppr^{d/-}$ mice is superficially very different from that of $Ppr^{-/-}$ mice. Close observations, however, revealed relative reductions of the periarticular and the columnar regions in $Ppr^{d/-}$ mice, which are also seen in $Ppr^{-/-}$ and *Col2-Cre:*$Ppr^{fl/fl}$ mice in extreme forms. The diminished extent of the periarticular region, despite increased proliferation in this region in both $Ppr^{d/-}$ and *Col2-Cre:*$Ppr^{fl/fl}$

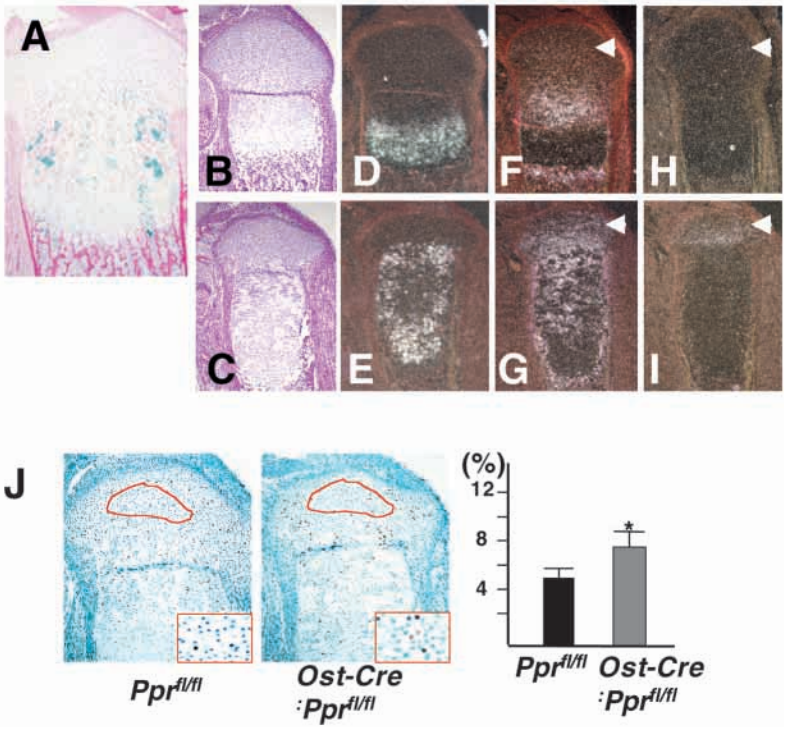

Fig. 6. Mosaic ablation of PPR in chondrocytes. (A) Mosaic activity of *Cre* recombinase of *Ost-Cre* transgenic mice in the growth plate. *Ost-Cre:R26R* doubly transgenic, an E17.5 embryo was stained with X-gal. β-gal activity was seen in about 30% of the columnar chondrocytes. β-gal-positive cells are few in the periarticular region. (B-I) In situ hybridization of E17.5 proximal tibias of $Ppr^{fl/fl}$ (B,D,F,H) and *Ost-Cre:*$Ppr^{fl/fl}$ (C,E,G,I). (D,E) *Ihh* is expressed in the hypertrophic region as well as ectopically differentiated hypertrophic cells in the *Ost-Cre:*$Ppr^{fl/fl}$ growth plate. (F,G) Expression of *Ptc* (F,G) and *Pthrp* (H,I) is upregulated in the periarticular region in the mutant growth plate (arrowheads). (J) BrdU labeling. Increased labeling ratio despite the small periarticular region in *Ost-Cre:*$Ppr^{fl/fl}$. The areas indicated by red lines were subjected to BrdU-positive cell counting. Insets are magnified views of the periarticular region. Nine sections from three animals of each genotype were counted. *P<0.01.

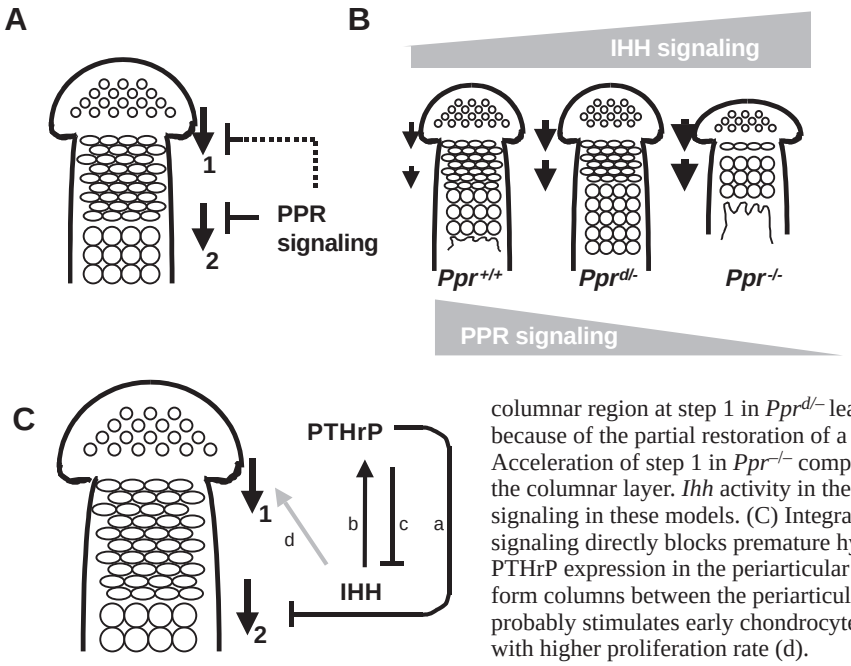

Fig. 7. Proposed model for the regulation of chondrocyte differentiation by PPR and Ihh signaling. (A) PPR signaling in the columnar chondrocytes blocks terminal differentiation (arrow 2). PPR signaling in chondrocytes also negatively controls the differentiation of periarticular chondrocytes to columnar chondrocytes (arrow 1). (B) Application of the model to mice with PPR mutations. Acceleration of cell supply to the columnar region at step 1 in $Ppr^{d/-}$ leads to an increase in hypertrophic cell production because of the partial restoration of a cell amplification step in the columnar layer. Acceleration of step 1 in $Ppr^{-/-}$ compensates for the loss of the cell amplification system in the columnar layer. *Ihh* activity in the periarticular region negatively correlates with PPR signaling in these models. (C) Integrated model of PTHrP/Ihh feedback loop. PTHrP signaling directly blocks premature hypertrophic differentiation (a). Ihh positively regulates PTHrP expression in the periarticular region (b). In the presence of PTHrP, chondrocytes form columns between the periarticular region and the Ihh-expressing domain (c). Ihh action probably stimulates early chondrocyte differentiation to increase chondrocyte population with higher proliferation rate (d).

mice, suggests that loss or impairment of PPR signaling accelerates the differentiation of periarticular cells to columnar cells. The BrdU study also excluded the possibility that an increase in proliferation of columnar cells might have caused the early hypertrophic expansion in the $Ppr^{d/-}$ growth plate. Thus, the expansion of the hypertrophic layer in the $Ppr^{d/-}$ mice is probably caused both by acceleration of differentiation of periarticular to columnar cells and acceleration of differentiation of columnar cells into hypertrophic cells. The former process supplies cells to the pool with the highest proliferation rate; therefore, modest acceleration of this step may cause a substantial difference in the production of hypertrophic cells, further abetted by early conversion of proliferating cells to hypertrophic cells. This combination of cell transformation causes the $Ppr^{d/-}$ mouse to have a tibia longer than normal at E17.5.

PTHrP expression in the periarticular region is dependent on Ihh expressed predominantly in the prehypertrophic chondrocytes. PTHrP, in turn, blocks premature hypertrophic differentiation of columnar chondrocytes (Kronenberg and Chung, 2001). However, Ihh clearly has roles in cartilage development independent of PTHrP, as $Ihh^{-/-}$ mice show a growth plate phenotype distinct from that of $Ppr^{-/-}$ mice, with marked reduction of chondrocyte proliferation. Expression of constitutively active PPR in the cartilage is able to reverse only acceleration of terminal differentiation of *Ihh*-null chondrocytes and is not able to rescue the reduced proliferation (Karp et al., 2000). The positive association between cellular proliferation and Ihh activity is also observed in periarticular chondrocytes of the different models presented here. The increased proliferation accompanies increased rates of differentiation of periarticular cells to columnar/hypertrophic cells.

Based on the observations above, we propose that alteration of PPR signaling in chondrocytes changes the rates of differentiation of periarticular to the columnar chondrocytes (arrow 1) as well as the generation of hypertrophic chondrocytes (arrow 2) (Fig. 7A). This model can explain the diversified phenotypes in various PPR mutant growth plates (Fig. 7B). However, the data from mosaic PPR ablation demonstrate that PPR signaling itself does not directly regulate the first step. Conversely, Ihh activity is positively correlated with the acceleration of the first step, along with an increase in proliferation, suggesting that Ihh action may positively control this step (Fig. 7C). There remains a possibility that another factor secreted from the ectopic hypertrophic chondrocytes might be responsible for this step. This possibility, however, appears unlikely because a previous study of chimeric growth plates composed of wild-type cells and $Ppr^{-/-};Ihh^{-/-}$ doubly mutant cells showed that Ihh in the ectopic hypertrophic chondrocytes was responsible for the characteristic elongation of the columnar layer of the growth plate (Chung et al., 2001).

Our study demonstrates that impairment of PPR signaling creates a novel growth plate phenotype. Through analysis of these mice, we have found that chondrocyte differentiation is controlled at multiple steps by the feedback loop of PTHrP and Ihh, and that Ihh probably stimulates differentiation of early chondrocytes. This process thus may increases a chondrocyte population with a high rate of proliferation.

We thank Dr En Li for providing us ES cells and Melissa Knight for technical assistance. This work was funded in part by NIH grants DK56246 and AR44855.

REFERENCES

Calvi, L. M., Sims, N. A., Hunzelman, J. L., Knight, M. C., Giovannetti, A., Saxton, J. M., Kronenberg, H. M., Baron, R. and Schipani, E. (2001). Activated parathytoid hormone/parathyroid hormone-related protein receptor in osteoblastic cells differentially affects cortical and trabecular bone. *J. Clin. Invest.* **107**, 277-286.

Chung, U., Lanske, B., Lee, K., Li, E. and Kronenberg, H. (1998). The parathyroid hormone/parathyroid hormone-related peptide receptor

coordinates endochondral bone development by directly controlling chondrocyte differentiation. *Proc. Natl. Acad. Sci. USA* **95**, 13030-13035.

Chung, U., Schipani, E., McMahon, A. P. and Kronenberg, H. M. (2001). Indian hedgehog couples chondrogenesis to osteogenesis in endochondral bone development. *J. Clin. Invest.* **107**, 295-304.

Frendo, J. L., Xiao, G., Fuchs, S., Franceschi, R. T., Karsenty, G. and Ducy, P. (1998). Functional hierarchy between two OSE2 elements in the control of osteocalcin gene expression in vivo. *J. Biol. Chem*. **273**, 30509-30516.

Go, C., He, W., Zhong, L., Li, P., Huang, J., Brinkley, B. R. and Wang, X. J. (2000). Aberrant cell cycle progression contributes to the early-stage accelerated carcinogenesis in transgenic epidermis expressing the dominant negative TGFbetaRII. *Oncogene* **19**, 3623-3631.

Goodrich, L. V., Johnson, R. L., Milenkovic, L., McMahon, J. A. and Scott, M. P. (1996). Conservation of the hedgehog/patched signaling pathway from flies to mice: Induction of a mouse patched gene by Hedgehog. *Genes Dev*. **10**, 301-312.

Karaplis, A. C., Luz, A., Glowacki, J., Bronson, R. T., Tybulewicz, V. L., Kronenberg, H. M. and Mulligan, R. C. (1994). Lethal skeletal dysplasia from targeted disruption of the parathyroid hormone-related peptide gene. *Genes Dev.* **8**, 277-289.

Karp, S. J., Schipani, E., St-Jacques, B., Hunzelman, J., Kronenberg, H. M. and McMahon, A. P. (2000). Indian hedgehog coordinates endochondral bone growth and morphogenesis via parathyroid hormone related-protein-dependent and -independent pathways. *Development*. **127**, 543-548.

Kronenberg, H. M. and Chung, U. (2001). The parathyroid hormone-related protein and Indian hedgehog feedback loop in the growth plate. *Novartis Found. Symp*. **232**, 144-152.

Lanske, B., Kraplis, A. C., Lee, K., Luz, A., Vortkamp, A., Pirro, A., Karperien, M., Defize, L. H., Ho, C., Mulligan, R. C. et al. (1996). PTH/PTHrP receptor in early development and Indian hedgehog-regulated bone growth. *Science* **273**, 663-666.

Lanske, B., Amling, M., Neff, L., Guiducci, J., Baron, R. and Kronenberg, H. M. (1999). Ablation of the PTHrP gene or the PTH/PTHrP receptor gene leads to distinct abnormalities in bone development. *J. Clin. Invest.* **104**, 399-407.

Lee, K., Deeds, J. and Segre, G. V. (1995). Expression of parathyroid hormone-related peptide and its receptor messenger ribonucleic acids during fetal development of rats. *Endocrinology* **136**, 453-463.

Meyers, E. N., Lewandoski, M. and Martin, G. R. (1998). An Fgf8 mutant allelic series generated by Cre- and Flp-mediated recombination. *Nat. Genet.* **18**, 136-141.

Mohn, A. R., Gainetdinov, R. R., Caron, M. G. and Koller, B. H. (1999). Mice with reduced NMDA receptor expression display behaviors related to schizophrenia. *Cell* **98**, 427-436.

Nagy, A., Moens, C., Ivanyi, E., Pawling, J., Gertsenstein, M., Hadjantonakis, A. K., Pirity, M. and Rossant, J. (1998). Dissecting the role of N-myc in development using a single targeting vector to generate a series of alleles. *Curr. Biol.* **8**, 661-664.

Nemir, M., Bhattacharyya, D., Li, X., Singh, K., Mukherjee, A. B. and Mukherjee, B. B. (2000). Targeted inhibition of osteopontin expression in the mammary gland causes abnormal morphogenesis and lactation deficiency. *J. Biol. Chem.* **275**, 969-976.

O'Gorman, S., Dagenais, N. A., Qian, M. and Marchuk, Y. (1997). Protamine-Cre recombinase transgenes efficiently recombine target sequences in the male germ line of mice, but not in embryonic stem cells. *Proc. Natl. Acad. Sci. USA* **23**, 14602-14607.

Pluck, A. (1996). Conditional mutagenesis in mice: the Cre/*loxP* recombination system *Int. J. Exp. Pathol.* **77**, 269-278.

Sauer, B. (1993). Manipulation of transgenes by site-specific recombination: Use of Cre reombinase. In *Guide to Techniques in Mouse Development* (ed. P. M. Wassarman, and M. L. DePamphilis), pp. 890-900. San Diego, CA: Academic Press.

Sauer, B. and Henderson, N. (1989). Cre-stimulated recombination at loxP-containing DNA sequences placed into the mammalian genome. *Nucleic Acids Res.* **17**, 147-161.

Schipani, E., Lanske, B., Hunzelman, J., Luz, A., Kovacs, C. S., Lee, K., Pirro, A., Kronenberg, H. M. and Juppner, H. (1997). Targeted expression of constitutively active receptors for parathyroid hormone and parathyroid hormone-related peptide delays endochondral bone formation and rescues mice that lack parathyroid hormone-related peptide. *Proc. Natl. Acad. Sci. USA* **94**, 13689-13694.

Schipani, E., Ryan, H. E., Didrickson, S., Kobayashi, T., Knight, M. and Johnson, R. S. (2001). Hypoxia in cartilage: HIF-1α is essential for chondrocyte growth arrest and survival. *Genes Dev*. **15**, 2865-2876.

Soriano, P. (1999). Generalized lacZ expression with the ROSA26 Cre reporter strain. *Nat. Genet.* **21**, 70-71.

St. Jacques, B., Hammerschmidt, M. and McMahon, A. P. (1999). Indian hedgehog signaling regulates proliferation and differentiation of chondrocytes and is essential for bone formation. *Genes Dev.* **13**, 2072-2086.

Tang, H. K., Chao, L. Y. and Saunders, G. F. (1997). Functional analysis of paired box missense mutations in the PAX6 gene. *Hum. Mol. Genet.* **6**, 381-386.

Vortkamp, A., Lee, K., Lanske, B., Segre, G. V., Kronenberg, H. M. and Tabin, C. (1996). Regulation of rate of cartilage differentiation by Indian hedgehog and PTH-related protein. *Science* **273**, 663-666.

Yamada, Y., Miyashita, T., Savagner, P., Horton, W., Brown, K. S., Abramczuk, J., Xie, H. X., Kohno, K., Bolander, M. and Bruggeman, L. (1990). Regulation of the collagen II gene in vitro and in transgenic mice. *Ann. New York Acad. Sci.* **580**, 81-87.